



# Optical photothermal infrared response (O-PTIR) of functionalized thiophene monomers and polymers

Quintin Baugh, Junghyun Lee, Yuhang Wu, Nurdan Cocuk, David C. Martin , Department of Materials Science and Engineering, The University of Delaware, Newark, USA

Address all correspondence to David C. Martin at [milty@udel.edu](mailto:milty@udel.edu)

(Received 6 May 2025; accepted 18 July 2025)

## Abstract

Optical photothermal infrared response (O-PTIR) spectroscopy is an emerging technique of particular interest for examining the local chemistry and structure of organic molecular and polymer materials. Here, we used O-PTIR to examine the 3,4-ethylenedioxythiophene (EDOT) and maleimide-functionalized (EDOT-MA) monomers, and also thin films (~100 nm) of their corresponding polymers (PEDOT and PEDOT-MA) electrochemically deposited on interdigitated (5 μm) gold electrodes. The O-PTIR technique provided high-resolution (~1 μm) information about the chemical structure, including the ability to map local variations in the composition of the MA side groups. Certain limitations were found, particularly in samples that were strongly optically absorbing.

## Introduction

PEDOT is an optically dark conjugated polymer that substantially improves the electrical capabilities of electrodes that are coated with it, particularly the charge transport properties (impedance) at low frequencies (less than ~10<sup>3</sup> Hz). Its optical absorbance and electrical conductivity stem from its conjugated π-bond network along the carbon backbone. It has been used for a variety of applications from electrochromic windows<sup>[1]</sup> to bioelectronic coatings.<sup>[2]</sup> PEDOT is chemically resilient, owing to the lack of reactive hydrogens along the conjugated backbone due to the presence of the dioxy-ring on the thiophene, allowing PEDOT coatings to be employed in a wide variety of chemical conditions with limited degradation. However, this chemical stability has a downside in that PEDOT is not easily chemically modified after deposition.<sup>[3]</sup> EDOT-MA is a chemically modified variant of the EDOT monomer that contains a maleimide subgroup covalently bonded to the dioxy-ring of the EDOT (Fig. 2). When polymerized, PEDOT-MA retains these maleimide subgroups, which may then be used for post-processing by way of the maleimide coupling click reactions<sup>[4]</sup> to reliably modify PEDOT coatings. These reactions likely predominantly involve the exposed surfaces of the PEDOT-MA, since the bulk maleimide groups would not be exposed to reaction medium, leading to a need to characterize these films through the changes in surface chemistry.

To fully exploit the PEDOT and PEDOT-MA films in applications, it is important to characterize their surfaces in a non-destructive manner such that we are able to differentiate reacted and unreacted species, and to confirm the success of any subsequent coupling reactions. This is not just a concern for maleimide-modified PEDOT-MA, but to any modified PEDOT that serves as a basis for post-processing, such as

azide-modified PEDOT films analyzed with XPS.<sup>[5]</sup> It is also a concern for any other polymer systems where local surface chemical modifications and control are desired. To this end, we make use of optical photothermal infrared response with complementary Raman spectroscopy to detect chemical changes at the surface of these films.

Optical Photothermal Infrared (O-PTIR) spectroscopy is an emerging technology used to measure the infrared and Raman spectra of materials. This method does not require an IR translucent substrate and serves as an excellent way to examine thick or otherwise cumbersome samples.<sup>[6,7]</sup> A visible laser of 532 nm is shone in tandem with a variable IR laser onto a sample. When the IR wavelength matches a vibrational mode of the bonds present within this sample is absorbed, the resulting photothermal expansion of the sample causes the elastic scattering of the coupled visible beam (Fig. 1).<sup>[8]</sup> This visible beam may also be used to generate the Raman spectrum of the same sample simultaneously to the IR spectrum collection through inelastic photon scattering.<sup>[9]</sup> The O-PTIR response for a given sample can be described with the following expression:

$$\Delta P_{\text{pr}} \propto \frac{\sigma N}{\kappa C_p} \frac{\partial n}{\partial T} P_{\text{pr}} P_{\text{IR}},$$

where  $P_{\text{pr}}$  is the probe power,  $\sigma$  is the absorption cross section,  $N$  is the number density,  $\kappa$  is the heat conductivity,  $C_p$  is the heat capacity,  $n$  is the refractive index,  $T$  is the temperature, and  $P_{\text{IR}}$  is the infrared power.<sup>[10]</sup> Due to the nature IR and visible beams used, the depth that O-PTIR is able to survey is dependent on the absorptive properties of the material in question. For instance, cellular and biological tissue samples are composed primarily of water and organic compounds, and while the visible beam is able to transmit through the water,

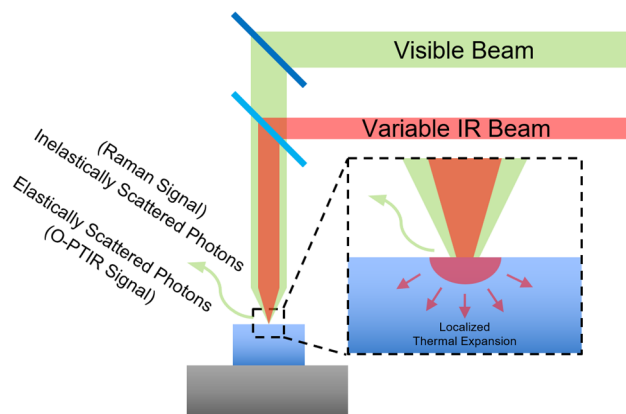


**Figure 1.** Cartoon diagram of the operation of O-PTIR microscopy involving simultaneous visible and infrared irradiation of a set point to produce elastically and inelastically scattered photons.

large portions of the IR spectrum will be readily absorbed, limiting the surveyable depth of biological tissues to be on the order of 10  $\mu\text{m}$ .<sup>[11,12]</sup> However, it has been found that the depth resolution of polymer films, while variable based on the surface roughness and chemical bonds present, can be as low as 1 nm.<sup>[13]</sup> Due to the highly absorptive optical properties and surface roughness of electrochemically deposited PEDOT films,<sup>[14]</sup> it is reasonable to assert that it would exhibit the same limit to the depth resolution of O-PTIR measurements as these other polymer films. To understand the value that O-PTIR provides, it is important to consider the fundamental differences between O-PTIR and other methods of obtaining IR spectra to understand its potential uses.

When comparing O-PTIR to other methods of obtaining IR spectra, several differences are observed due to both physical and instrumental limitations. Transmission FTIR is the standard way of obtaining IR spectra from samples and

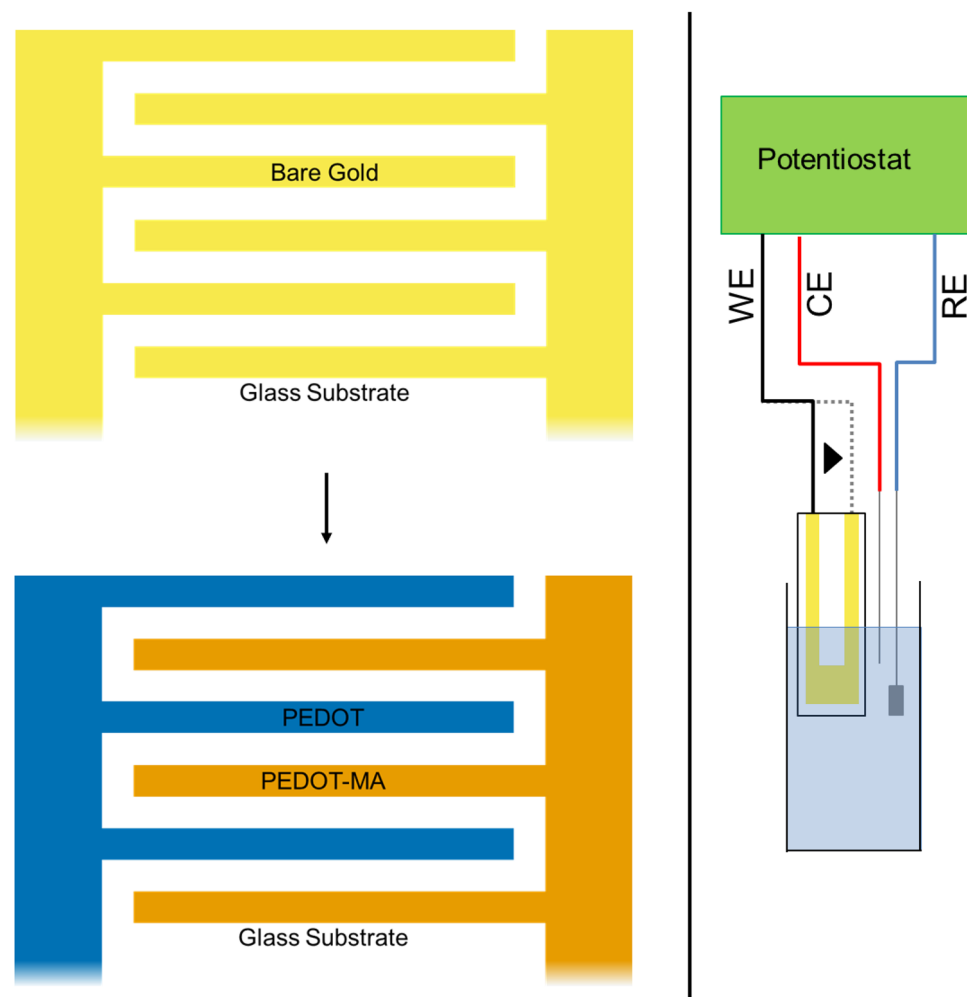


**Figure 2.** **Left:** Schematic of PEDOT and PEDOT-MA deposition on an interdigitated gold electrode highlighting the complete separation of both PEDOT variants. **Right:** Schematic representation of the electrodeposition setup used to polymerize PEDOT (blue) and PEDOT-MA (orange) on both sets of interdigitated electrodes. WE: Working Electrode, CE: Counter Electrode, RE: Reference Electrode.

involves passing infrared light through a sample to analyze the amount of light that the sample absorbs. This technique is relatively simple, and the IR spectra may be obtained over large ranges (e.g., 4000–650  $\text{cm}^{-1}$ ). However, there are limitations in the kinds of samples that can be analyzed, as they must be either suspended in a solvent that is transparent over the window of IR wavelengths of interest, or be thin enough to remain translucent when placed in the beam path.<sup>[15]</sup> It is for these reasons that this method is unsuitable for opaque, thick, and/or layered films with heterogeneous compositions, where individual layers must be characterized. Attenuated Total Reflection Fourier Transform Infrared Spectroscopy (ATR-FTIR) is a method that makes use of a single crystal to which the sample is brought into contact. Infrared light is then totally internally reflected within this crystal and an evanescent wave interacts with the sample interface, producing the IR spectrum of the sample from the light that is reflected back over ranges similar to transmission FTIR. The penetration depth  $d_p$  of ATR-FTIR is generally on the order of a few micrometers, and is a function of the evanescent wave interaction with the incident light and the sample. It is defined as follows:

$$d_p = \frac{\lambda}{2\pi n_r \sqrt{\sin^2 \theta - \frac{n^2}{n_r^2}}},$$

where  $\lambda$  is the wavelength of light,  $\theta$  is the angle of incident light,  $n_r$  is the refractive index of the crystal, and  $n$  is the refractive index of the sample.<sup>[16]</sup> Due to the limited penetration depth, this method lends itself to examining thin films and coatings, with the limitation that such films and coatings must be directly applied to the crystal used in the instrument, with layered films being equally unapproachable to transmission FTIR, and with both transmission FTIR and ATR-FTIR sharing similar spatial resolutions on the order of 10  $\mu\text{m}$ .<sup>[17]</sup> Atomic force microscopy with photothermal infrared spectroscopy (AFM-PTIR) is a method similar to O-PTIR that makes use of the same photothermal properties, but analyzes the physical deflection of a mechanical probe instead of the scattering of an optical probe. As it observes the same physical properties of a sample, AFM-PTIR shares the same profiling depth and limited IR range of O-PTIR (e.g., 1800–800  $\text{cm}^{-1}$ ), with the added limitations that the mechanical probe cannot easily monitor rough, highly heterogeneous, or liquid surfaces, while also adding the risk of mechanically damaging the sample. While the spatial resolution of AFM-PTIR is cantilever dependent and on the order of 1  $\mu\text{m}$ , it can be used for microscale applications, contrasting with O-PTIR which boasts a spatial resolution on the order of 0.5  $\mu\text{m}$ .<sup>[18]</sup>

Several standard polymers have been analyzed with O-PTIR and coupled Raman spectroscopy to compare the results with more traditional acquisition methods. Polyethylene (PE), polypropylene (PP), polyvinyl chloride (PVC), polyethylene terephthalate (PET), polycarbonate (PC), polystyrene (PS), polyactic

acid (PLA), polymethylmethacrylate (PMMA), and silicone were comparatively analyzed using O-PTIR and ATR-FTIR for IR spectral comparisons over the 1800–800  $\text{cm}^{-1}$  range, and with O-PTIR coupled Raman and regular Raman spectroscopy for Raman spectral comparisons over the 1800–250  $\text{cm}^{-1}$  range.<sup>[19]</sup> All polymers showed nearly overlapping IR peak positions between methods, but with moderately variable intensities being observed. As PET contains similar chemical groups to EDOT and EDOT-MA, its results will be specifically described here. PET showed overlapping peak positions at 872  $\text{cm}^{-1}$ , 1018  $\text{cm}^{-1}$ , 1097  $\text{cm}^{-1}$ , and 1409  $\text{cm}^{-1}$ , but showed slight shifts in the 1246  $\text{cm}^{-1}$  and 1716  $\text{cm}^{-1}$  peaks, with the 872  $\text{cm}^{-1}$  and 1716  $\text{cm}^{-1}$  peaks being at similar intensities, 1097  $\text{cm}^{-1}$  and 1409  $\text{cm}^{-1}$  peaks having higher O-PTIR intensities compared to ATR-FTIR, and the 1018  $\text{cm}^{-1}$  and 1246  $\text{cm}^{-1}$  peaks having lower O-PTIR intensities compared to ATR-FTIR. As for Raman spectroscopy, all polymers showed nearly overlapping peak positions in all cases, but with O-PTIR having higher intensities in nearly all cases. For PET, O-PTIR and ATR-FTIR were in close agreement in terms of peak position and peak intensity for the 632  $\text{cm}^{-1}$ , 857  $\text{cm}^{-1}$ , 1287  $\text{cm}^{-1}$ , 1614  $\text{cm}^{-1}$ , and 1725  $\text{cm}^{-1}$  peaks presented.<sup>[19]</sup>

In this study, we expand on the work of polymer characterization and make use of O-PTIR microscopy to characterize and differentiate electrochemically deposited PEDOT and PEDOT-MA coatings on a microelectronic device. Both EDOT and EDOT-MA monomers are characterized using IR and Raman spectroscopy, before then depositing polymer forms of both onto two separated sets of electrodes. The presence of both films are independently verified through electrochemical impedance spectroscopy, with the chemical differences between PEDOT and PEDOT-MA being determined using surface IR and Raman spectroscopy.

## Experimental methods

### Electrochemical polymerization

All electrochemical polymerizations were performed on a Metrohm Autolab PGSTAT128N potentiostat using a three-electrode setup, where the working electrode was one side of a Metrohm 5  $\mu\text{m}$  interdigitated gold electrode (G-IDEAU5), the counter electrode was a platinum wire (Surepure Chemetals), and the reference electrode was a Ag/AgCl pellet (Warner Instruments) (Fig. 2).<sup>[20]</sup> Monomer solutions consisted of 10 mM of either EDOT (Sigma-Aldrich) or EDOT-MA<sup>[21]</sup> respective to their designated electrode, and 20 mM  $\text{LiClO}_4$  (Sigma-Aldrich) in DI water provided by a MilliporeSigma Milli-Q Reference Ultrapure Water Purification System for EDOT, and acetonitrile (Sigma-Aldrich) for EDOT-MA. Polymerization was handled using a galvanostatic (constant current) method at 75  $\mu\text{A}$  with a target charge density of 0.01  $\text{C}/\text{cm}^2$  applied to the total working electrode area of  $8.45 \times 10^{-2}$   $\text{cm}^2$  for the electrode geometry used. Electrochemical Impedance Spectroscopy (EIS) over a frequency range of  $10^{-1}$  Hz to

$10^5$  Hz was performed before and after this procedure using the same electrode setup with a 0.1 M NaCl electrolyte solution.

### Photothermal infrared imaging

All IR and Raman spectra were taken using a Photothermal Infrared mIRage instrument with IR spectra taken between 1924 and  $790\text{ cm}^{-1}$  and Raman spectra taken between  $500$  and  $3700\text{ cm}^{-1}$  due to the configuration of the instrument.<sup>[17]</sup> All measurements were taken using a standard detector with same-day background calibration and a 5X gain.

### Monomer examination

EDOT and EDOT-MA monomers were examined for their IR and Raman spectra. A droplet of EDOT was placed on a glass slide, and had an IR spectrum taken using 22% IR power and a Raman spectrum taken using 25% probe power with a  $65\text{ }\mu\text{m}$  confocal pinhole. EDOT-MA powder was then placed on a glass slide and similarly had IR and Raman spectra taken using the same settings as for the EDOT droplet.

### Polymer examination

PEDOT and PEDOT-MA-coated IDE as prepared previously were examined with both PEDOT and PEDOT-MA having Raman spectra taken at 50% IR power and 7% probe power with a  $65\text{-}\mu\text{m}$  confocal pinhole, respectively. An IR surface map was then taken over a  $60\text{ }\mu\text{m} \times 10\text{ }\mu\text{m}$  area across 6 digits of the IDE at  $1718\text{ cm}^{-1}$ .

## Results

Due to the interfacial surface modification of these polymer films, it was necessary to explore surface characterization methods to differentiate chemical modifications. Bulk characterization methods as well as destructive characterization methods would be unusable in these cases, as the modified surface of a film would compose far less of the total material than the internal bulk material would. Likewise, destructive characterization methods would destroy the surface intended to be characterized and only provide characterization of the underlying surface. It is for these reasons that surface infrared and Raman spectroscopy are so attractive for this application, as it is a minimally penetrative and non-destructive characterization method for differentiating chemical components of film surfaces.

By first examining the monomers, spectral properties and differences between the two may be found that would show the properties expected in polymerized samples. By comparing the IR spectra of EDOT and EDOT-MA, several key similarities and differences may be seen (Fig. 3). First and foremost, EDOT-MA shows a large peak at  $1718\text{ cm}^{-1}$  from the carbonyl groups present in the maleimide<sup>[22]</sup> that is completely absent from the EDOT. Also, the moderate peak present at  $1492\text{ cm}^{-1}$  shows the presence of thiophene aromatic carbons in both EDOT and EDOT-MA, with the base EDOT spectrum being

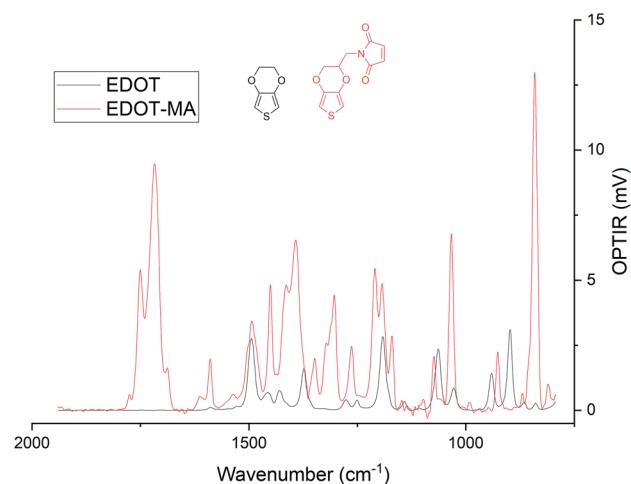


**Figure 3.** Infrared comparison of EDOT and EDOT-MA.

**Table 1.** Key peak assignments for EDOT and EDOT-MA IR comparison.

Wavenumber ( $\text{cm}^{-1}$ )	Assignment
1718	Maleimide Carbonyl C=O
1492	Thiophene Aromatic Carbons
1391	Maleimide Linker $\text{CH}_2$
1065	EDOT Ether C–O–C
841	Maleimide Alkene C=C

similar to what has previously been reported<sup>[23,24]</sup> (Table 1). The similarities between EDOT and EDOT-MA are consistent with their molecular structures, and with polymers with similar chemical groups analyzed previously, namely the aromatic carbons and C=O present in PET.<sup>[19]</sup> EDOT-MA is a modified EDOT monomer, and shows similar traits to EDOT while also showing the traits of the maleimide addition. The conclusions found from the monomer IR spectral comparison extended to the IR mapping of the double-polymer-coated interdigitated electrode, in which a clear difference could be seen in the optical photothermal infrared response of the two polymers scanned at  $1718\text{ cm}^{-1}$  [Fig. 4(a)].

This image clearly shows the ability of the O-PTIR technique to map out local chemical compositions of the PEDOT and PEDOT-MA film deposited on the interdigitated gold electrodes. The broadening signal near the edges of the electrode is due to PEDOT growing out and away from the electrodes, but due to the overlap of the stronger O-PTIR signal with the bounds of the electrode, we estimate the effective resolution of the technique as approximately  $1\text{ }\mu\text{m}$ .

The electrodeposition of PEDOT and PEDOT-MA led to a drop in the low-frequency impedance of approximately 2 orders of magnitude for both coated electrodes [Fig. 4(b)]. This drop in impedance is consistent with the previous observations of similar coatings.<sup>[21]</sup> These coatings were thin, with an estimated

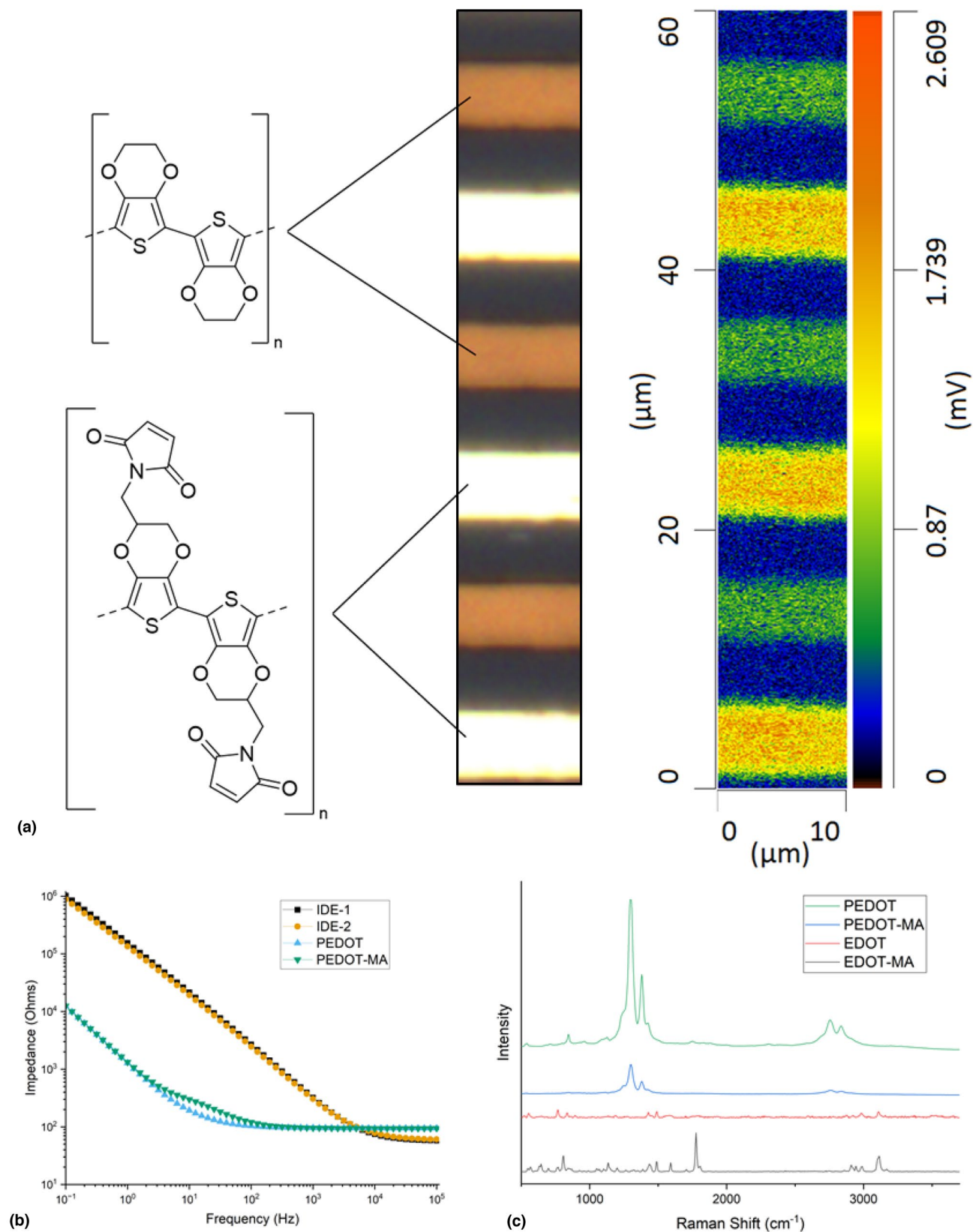


**Figure 4.** (a) **Center:** Reflected optical microscopy image of the coated interdigitated electrode. Lightest bands are PEDOT-MA-coated electrodes, brown bands are PEDOT-coated electrodes, and darkest bands are uncoated glass substrate. (a) **Right:** O-PTIR mapping of area depicted in the center image. (b): Electrochemical Impedance Spectroscopy of PEDOT and PEDOT-MA-coated IDE. (c): Raman comparison of (P)EDOT and (P)EDOT-MA **C:** IR Mapping for PEDOT and PEDOT-MA at  $1718\text{ cm}^{-1}$ .

**Table II.** Raman key peak assignments for (P)EDOT and (P)EDOT-MA comparison.

Wavenumber (cm <sup>-1</sup> )	Assignment
1428	PEDOT C <sub>α</sub> =C <sub>β</sub> (-O)
1773	Maleimide Carbonyl C-C=O
2864	PEDOT CH <sub>2</sub>

thickness of 24 nm for PEDOT and 120 nm for PEDOT-MA based on the total charge density and other studies from our laboratory,<sup>[25]</sup> and as seen by the trace electrode color changes observed optically throughout the polymerization process.

The Raman spectra taken from both the monomers and polymers can be compared to complement the IR spectra and show a greater level of detail between the (P)EDOT and (P)EDOT-MA [Fig. 4(c)]. The monomers showed clear differences related to the presence of the maleimide on the EDOT-MA and absent on the EDOT, as shown mostly through the peaks at 1773 cm<sup>-1</sup> present in EDOT-MA but completely absent in EDOT. This peak is directly related to the presence of the carbonyl groups in the maleimide present in EDOT-MA.<sup>[26,27]</sup> PEDOT and PEDOT-MA also showed key differences to their monomers in the form of peak clusters at 1428 cm<sup>-1</sup> and 2864 cm<sup>-1</sup> (Table II), which are peaks strongly associated with the presence of PEDOT.<sup>[28,29]</sup> However, the 1773 cm<sup>-1</sup> peak associated with the maleimide present in EDOT-MA was not present in the Raman spectrum of PEDOT-MA, indicating that Raman spectral analysis by O-PTIR is insufficient to detect these kinds of chemical changes on the surfaces of the polymer. This is reasonable considering the dual-beam nature of the O-PTIR method. The infrared beam was likely able to pierce below the surface of the PEDOT film and be absorbed by maleimide present there, causing at least some thermal expansion and elastic photon scattering that was unimpeded by the PEDOT chains themselves. However, the visible beam from the Raman laser was likely overwhelmingly absorbed by the PEDOT chains at these same depths, preventing the visible light from hitting much of the maleimide present. Those photons that did inelastically scatter from the maleimide would then have to go back through any overlaying PEDOT, diminishing the maleimide Raman signal overall. This explains the discrepancy between the findings of PEDOT and PEDOT-MA here and the findings with other non-conjugated polymers in the literature. For PET, both carbonyl and aromatic carbons are present in the IR and Raman spectra collected using O-PTIR,<sup>[19]</sup> however, PET does not have any extended pi-bond conjugation and thus would have limited visible light interaction as opposed to the conjugated nature of PEDOT and PEDOT-MA. It is for this reason that depth resolution is largely insignificant when investigating pure materials that do not absorb visible light to a large degree.

## Conclusions

The construction of electrochemically deposited thin PEDOT and PEDOT-MA films were characterized through O-PTIR microscopy to compare surface IR and Raman spectra between PEDOT variants and their respective monomers. Both polymers showed considerable increases in their Raman spectra at 1428 cm<sup>-1</sup> and 2864 cm<sup>-1</sup> compared to their monomer counterparts due to the extended  $\pi$ -bond conjugation present. The IR spectrum of EDOT-MA also showed the addition of a large peak at 1718 cm<sup>-1</sup> compared to EDOT due to the chemical addition of the maleimide carbonyl groups. When the PEDOT and PEDOT-MA polymers were scanned to create a surface IR map at this wavelength, polymer-wide contrast was able to be detected. The ability for the IR scan to detect the maleimide while the Raman spectra could not is likely due to the relationship between the O-PTIR method itself and the surface properties of the PEDOT polymers. The surface roughness of the PEDOT polymer coatings along with the highly optically absorptive nature of PEDOT likely reduces the penetrative capabilities of the visible beam probe of the O-PTIR instrument, limiting its surveying depth to the order of a nanometer. This allows the PEDOT to produce a strong Raman signal while the maleimide signal is suppressed. The IR beam of the O-PTIR instrument would not be limited in this way, and would only need to heat up maleimide groups enough to cause enough thermal expansion in the surrounding PEDOT to produce the signal that is seen. The absorption coefficient of PEDOT at this wavenumber is reported to be approximately 50,000 cm<sup>-1</sup>,<sup>[30]</sup> corresponding to a penetration depth of ~200 nm. This is reasonably consistent with both previous work concerning PEDOT thickness control relating to optical darkness and the results from this study. PEDOT and PEDOT-MA have highly complex surface morphologies, and it is reasonable to assert that the penetration depth of the IR beam would allow it to cross multiple surface interfaces present through the film.

The ability to detect surface chemistry alterations of PEDOT-coated electrodes has thus been found to be sufficiently possible through O-PTIR characterization, as shown through the detection of carbonyl bonds present in maleimide subgroups being found in PEDOT-MA-coated electrodes, but not PEDOT-coated ones. This is reinforced by the IR analysis of the respective monomers, which show a similar difference in features. However, Raman spectroscopy was insufficient in determining differences in surface chemistry, for while the monomers did indeed show a difference in spectra, this was not observed in the polymer film characterization.

Further work in the chemical characterization of thin film interfaces like these could take the form of chemically reactive assays to verify the presence of post-processing products, or QCM/SPR studies to determine surface mass accumulation in the presence of analytes. Alternatively prepared PEDOT films could also be tested to investigate the role of surface morphology on the ability of O-PTIR to probe for surface IR and Raman spectra. Such methods would preserve the integrity of

the surface conditions, while also giving insight into the chemical properties of the surfaces.

## Acknowledgments

The authors would like to thank the University of Delaware's Advanced Materials Characterization Lab (AMCL) for access to the equipment used for this study, as well as Dr. Gerald Poirier and Dr. Jing Qu for training and assistance.

## Author contributions

Quintin Baugh performed the procedures and analytical techniques used to produce the results. Junghyun Lee assisted with the electrochemical deposition of the polymer films. Junghyun Lee, Yuhang Wu, and Nurdan Cocuk contributed to writing the document and giving feedback. David Martin reviewed the document and the work contained therein and provided feedback.

## Funding

Funding was provided through the University of Delaware's discretionary fund given to David Martin, as well as by the Waters Corporation through their Immerse Delaware fund.

## Data availability

The authors declare that the data used in the analysis shown in this study are provided within the paper. Should any data files be needed, they will be provided by the corresponding author upon reasonable request.

## Declarations

### Conflict of interest

On behalf of all authors, the corresponding author states that there is no conflict of interest.

## Supplementary Information

The online version contains supplementary material available at <https://doi.org/10.1557/s43579-025-00783-0>.

## Open Access

This article is licensed under a Creative Commons Attribution 4.0 International License, which permits use, sharing, adaptation, distribution and reproduction in any medium or format, as long as you give appropriate credit to the original author(s) and the source, provide a link to the Creative Commons licence, and indicate if changes were made. The images or other third party material in this article are included in the article's Creative Commons licence, unless indicated otherwise in a credit line to the material. If material is not included in the article's

Creative Commons licence and your intended use is not permitted by statutory regulation or exceeds the permitted use, you will need to obtain permission directly from the copyright holder. To view a copy of this licence, visit <http://creativecommons.org/licenses/by/4.0/>.

## References

- Z.D. Marks, D. Glugla, J.T. Friedlein, S.E. Shaheen, R.R. McLeod, M.Y. Kahook, D.P. Nair, Switchable diffractive optics using patterned PEDOT:PSS based electrochromic thin-films. *Org. Electron.* **37**, 271–279 (2016). <https://doi.org/10.1016/j.orgel.2016.07.004>
- C. Slaughter, S. Velasco-Bosom, X. Tao, R. Ruiz-Mateos Serrano, S. Kissovsky, R. Mizuta, D. Mantione, S.T. Keene, G.G. Malliaras, A. Dominguez-Alfaro, Electrogelation of PEDOT:PSS and its copolymer for bioelectronics. *J. Mater. Chem. C* **12**(37), 14944–14954 (2024). <https://doi.org/10.1039/D4TC02908A>
- O.A. Guselnikova, P.S. Postnikov, P. Fiti, D. Tomecek, P. Sajdl, R. Elashnikov, Z. Kolska, M.M. Chehimi, V. Švorčík, O. Lyutakov, Tuning of PEDOT:PSS properties through covalent surface modification. *J. Polym. Sci. B Polym. Phys.* **55**(4), 378–387 (2017). <https://doi.org/10.1002/polb.24282>
- B.H. Northrop, S.H. Frayne, U. Choudhary, Thiol-maleimide “click” chemistry: evaluating the influence of solvent, initiator, and thiol on the reaction mechanism, kinetics, and selectivity. *Polym. Chem.* **6**(18), 3415–3430 (2015). <https://doi.org/10.1039/C5PY00168D>
- J.U. Lind, T.S. Hansen, A.E. Daugaard, S. Hvilsted, T.L. Andresen, N.B. Larsen, Solvent composition directing click-functionalization at the surface or in the bulk of azide-modified PEDOT. *Macromolecules* **44**(3), 495–501 (2011). <https://doi.org/10.1021/ma102149u>
- A. Razumtcev, M. Li, J. Rong, C.C. Teng, C. Pfluegl, L.S. Taylor, G.J. Simpson, Label-free autofluorescence-detected mid-infrared photothermal microscopy of pharmaceutical materials. *Anal. Chem.* **94**(17), 6512–6520 (2022). <https://doi.org/10.1021/acs.analchem.1c05504>
- A. Spadea, J. Denbigh, M.J. Lawrence, M. Kansiz, P. Gardner, Analysis of fixed and live single cells using optical photothermal infrared with concomitant Raman spectroscopy. *Anal. Chem.* **93**(8), 3938–3950 (2021). <https://doi.org/10.1021/acs.analchem.0c04846>
- N.E. Olson, Y. Xiao, Z. Lei, A.P. Ault, Simultaneous optical photothermal infrared (O-PTIR) and Raman spectroscopy of submicrometer atmospheric particles. *Anal. Chem.* **92**(14), 9932–9939 (2020). <https://doi.org/10.1021/acs.analchem.0c01495>
- A. Paolone, A. Celeste, M. Di Pea, S. Brutti, F. Borondics, F. Capitani, A 3D printed air-tight cell adaptable for far-infrared reflectance, optical photothermal infrared spectroscopy, and Raman spectroscopy measurements. *Instruments* **8**(4), 54 (2024). <https://doi.org/10.3390/instrument8040054>
- D. Zhang, C. Li, C. Zhang, M.N. Slipchenko, G. Eakins, J.-X. Cheng, Depth-resolved mid-infrared photothermal imaging of living cells and organisms with submicrometer spatial resolution. *Sci. Adv.* **2**(9), e1600521 (2016). <https://doi.org/10.1126/sciadv.1600521>
- A. Paulus, S. Yogarasa, M. Kansiz, I. Martinsson, G.K. Gouras, T. Deierborg, A. Engdahl, F. Borondics, O. Klementieva, Correlative imaging to resolve molecular structures in individual cells: substrate validation study for super-resolution infrared microspectroscopy. *Nanomed. Nanotechnol. Biol. Med.* **43**, 102563 (2022). <https://doi.org/10.1016/j.nano.2022.102563>
- C. Prater, Y. Bai, S.C. Konings, I. Martinsson, V.S. Swaminathan, P. Nordenfelt, G. Gouras, F. Borondics, O. Klementieva, Fluorescently guided optical photothermal infrared microspectroscopy for protein-specific bioimaging at subcellular level. *J. Med. Chem.* **66**(4), 2542–2549 (2023). <https://doi.org/10.1021/acs.jmedchem.2c01359>
- J. Yu, Y. Xing, Z. Shen, Y. Zhu, D. Neher, N. Koch, G. Lu, Infrared spectroscopy depth profiling of organic thin films. *Mater. Horiz.* **8**(5), 1461–1471 (2021). <https://doi.org/10.1039/D0MH02047H>

14. Y. Xiao, X. Cui, D.C. Martin, Electrochemical polymerization and properties of PEDOT/S-EDOT on neural microelectrode arrays. *J. Electroanal. Chem.* **573**(1), 43–48 (2004). <https://doi.org/10.1016/j.jelechem.2004.06.024>
15. D.I. Sánchez-Machado, J. López-Cervantes, A.A. Escárcega-Galaz, O.N. Campas-Baypoli, D.M. Martínez-Ibarra, S. Rascón-León, Measurement of the degree of deacetylation in chitosan films by FTIR, <sup>1</sup>H NMR and UV spectrophotometry. *Methods X* **12**, 102583 (2024). <https://doi.org/10.1016/j.mex.2024.102583>
16. J. Grdadolnik, ATR-FTIR spectroscopy: its advantages and limitations. *Acta Chim. Slov.* **49**(3), 631–642 (2002)
17. M. Kansiz, C. Prater, E. Dillon, M. Lo, J. Anderson, C. Marcott, A. Demissie, Y. Chen, G. Kunkel, Optical photothermal infrared microspectroscopy with simultaneous Raman – a new non-contact failure analysis technique for identification of <10 Mm organic contamination in the hard drive and other electronics industries. *Micros. Today* **28**(3), 26–36 (2020). <https://doi.org/10.1017/S1551929520000917>
18. C. Molina, D. Kim, L. Mehndiratta, J. Lee, C.K. Madawala, J.H. Slade, A.V. Tivanski, V.H. Grassian, Comparison of different vibrational spectroscopic probes (ATR-FTIR, O-PTIR, Micro-Raman, and AFM-IR) of lipids and other compounds found in environmental samples: case study of substrate-deposited sea spray aerosols. *ACS Meas. Sci. Au* **5**(1), 74–86 (2025). <https://doi.org/10.1021/acsmesuresciau.4c00033>
19. J.S. Böke, J. Popp, C. Krafft, Optical photothermal infrared spectroscopy with simultaneously acquired raman spectroscopy for two-dimensional microplastic identification. *Sci. Rep.* **12**(1), 18785 (2022). <https://doi.org/10.1038/s41598-022-23318-2>
20. J. Lee, S. Chhatre, P. Sitarik, Y. Wu, Q. Baugh, D.C. Martin, Electrochemical fabrication and characterization of organic electrochemical transistors using poly(3,4-ethylenedioxythiophene) with various counterions. *ACS Appl. Mater. Interfaces* **14**(37), 42289–42297 (2022). <https://doi.org/10.1021/acsmi.2c10149>
21. S. Nagane, P. Sitarik, Y. Wu, Q. Baugh, S. Chhatre, J. Lee, D.C. Martin, Functionalized polythiophene copolymers for electronic biomedical devices. *MRS Advances* **5**(18–19), 943–956 (2020). <https://doi.org/10.1557/adv.2020.3>
22. E.C. Aguiar, J.B.P. Da Silva, M.N. Ramos, A theoretical study of the vibrational spectrum of maleimide. *J. Mol. Struct.* **993**(1–3), 431–434 (2011). <https://doi.org/10.1016/j.molstruc.2010.10.042>
23. P. Damlin, C. Kvarnström, A. Ivaska, Electrochemical synthesis and in situ spectroelectrochemical characterization of poly(3,4-ethylenedioxythiophene) (PEDOT) in room temperature ionic liquids. *J. Electroanal. Chem.* **570**(1), 113–122 (2004). <https://doi.org/10.1016/j.jelechem.2004.03.023>
24. C. Kvarnström, H. Neugebauer, S. Blomquist, H.J. Ahonen, J. Kankare, A. Ivaska, In situ spectroelectrochemical characterization of poly(3,4-ethylenedioxythiophene). *Electrochim. Acta* **44**(16), 2739–2750 (1999). [https://doi.org/10.1016/S0013-4686\(98\)00405-8](https://doi.org/10.1016/S0013-4686(98)00405-8)
25. Lee, J. Electrochemical Fabrication and Characterization of Organic Electrochemical Transistors. University of Delaware, 2024.
26. J. Aramendia, L. Gomez-Nubla, M.L. Tuite, K.H. Williford, K. Castro, J.M. Madariaga, A new semi-quantitative surface-enhanced raman spectroscopy (SERS) method for detection of maleimide (2,5-pyrroledione) with potential application to astrobiology. *Geosci. Front.* **12**(5), 101226 (2021). <https://doi.org/10.1016/j.gsf.2021.101226>
27. T. Woldbæk, P. Klaboe, C.J. Nielsen, The vibrational spectra of maleimide and N-D maleimide. *J. Mol. Struct.* **27**(2), 283–301 (1975). [https://doi.org/10.1016/0022-2860\(75\)87037-2](https://doi.org/10.1016/0022-2860(75)87037-2)
28. S. Garreau, G. Louarn, J.P. Buisson, G. Froyer, S. Lefrant, In situ spectroelectrochemical raman studies of Poly(3,4-ethylenedioxythiophene) (PEDT). *Macromolecules* **32**(20), 6807–6812 (1999). <https://doi.org/10.1021/ma9905674>
29. T.P. Nguyen, P. Le Rendu, P.D. Long, S..A. De Vos, Chemical and thermal treatment of PEDOT:PSS thin films for use in organic light emitting diodes. *Surf. Coat. Technol.* **180–181**, 646–649 (2004). <https://doi.org/10.1016/j.surfcoat.2003.10.110>
30. J. Hwang, D.B. Tanner, I. Schwendeman, J.R. Reynolds, Optical properties of nondegenerate ground-state polymers: three dioxothiophene-based conjugated polymers. *Phys. Rev. B* **67**(11), 115205 (2003). <https://doi.org/10.1103/PhysRevB.67.115205>

**Publisher's Note** Springer Nature remains neutral with regard to jurisdictional claims in published maps and institutional affiliations.